Joule

CellPress

Article

Innovative Chemicals and Materials from Bacterial Aromatic Catabolic Pathways

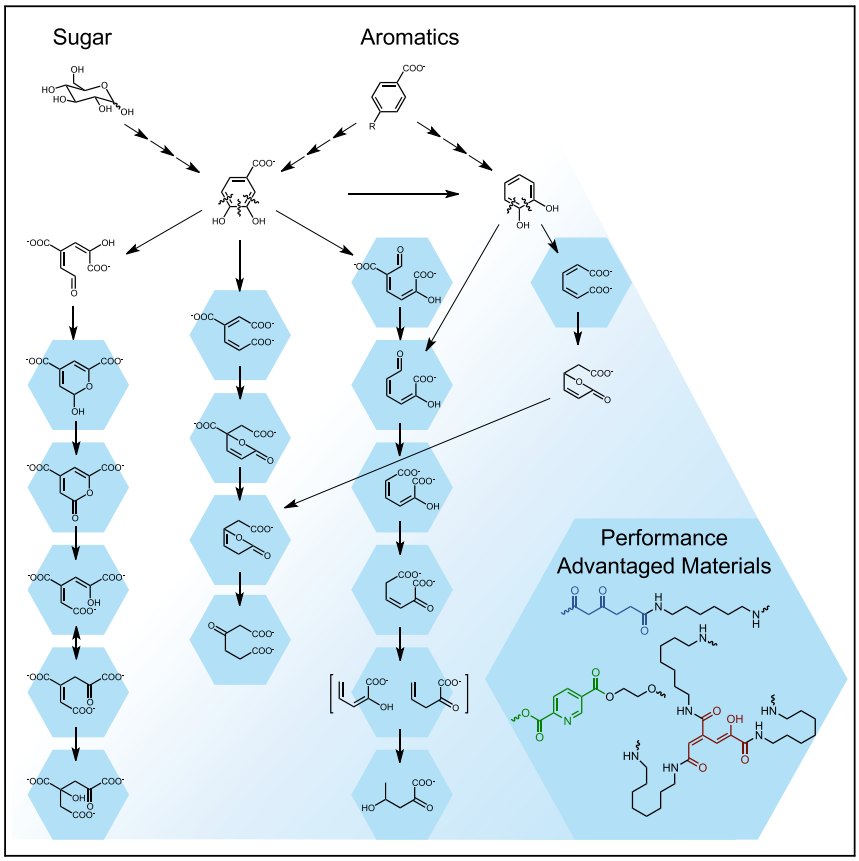

Intermediates of bacterial aromatic catabolism contain chemical functionality that could enable them to serve as precursors to environmentally compatible materials with similar or superior properties relative to petroleum-derived incumbents. Here, *Pseudomonas putida* was engineered to convert aromatic molecules and glucose into 16 of these metabolic intermediates including muconic acid, which was produced at a 41% yield from glucose. Several of these molecules were then polymerized to generate performance-advantaged materials.

Christopher W. Johnson, Davinia Salvachúa, Nicholas A. Rorrer, ..., Yannick J. Bomble, Adam M. Guss, Gregg T. Beckham

gregg.beckham@nrel.gov

HIGHLIGHTS

Pseudomonas putida was engineered to produce 16 intermediates of aromatic catabolism

Production of these molecules was demonstrated from aromatic compounds and glucose

Metabolic modeling and strain engineering achieved 41% yield of muconic acid from glucose

Polymerization of these molecules generated performance-advantaged materials

Johnson et al., Joule *3*, 1523–1537
June 19, 2019
https://doi.org/10.1016/j.joule.2019.05.011

Joule

CellPress

Article

Innovative Chemicals and Materials from Bacterial Aromatic Catabolic Pathways

Christopher W. Johnson,[1,7] Davinia Salvachúa,[1,7] Nicholas A. Rorrer,[1,7] Brenna A. Black,[2,7] Derek R. Vardon,[1,7] Peter C. St. John,[2,7] Nicholas S. Cleveland,[1] Graham Dominick,[1,4] Joshua R. Elmore,[3,5] Nicholas Grundl,[1] Payal Khanna,[1,6] Chelsea R. Martinez,[1] William E. Michener,[2] Darren J. Peterson,[2] Kelsey J. Ramirez,[2] Priyanka Singh,[1] Todd A. VanderWall,[2] A. Nolan Wilson,[1] Xiunan Yi,[1] Mary J. Biddy,[2] Yannick J. Bomble,[2] Adam M. Guss,[3] and Gregg T. Beckham[1,8,*]

SUMMARY

To drive innovation in chemical and material applications beyond what has been afforded by the mature petrochemical industry, new molecules that possess diverse chemical functionality are needed. One source of such molecules lies in the varied metabolic pathways that soil microbes utilize to catabolize aromatic compounds generated during plant decomposition. Here, we have engineered *Pseudomonas putida* KT2440 to convert these aromatic compounds to 15 catabolic intermediates that exhibit substantial chemical diversity. Bioreactor cultivations, analytical methods, and bench-scale separations were developed to enable production (up to 58 g/L), detection, and purification of each target molecule. We further engineered strains for production of a subset of these molecules from glucose, achieving a 41% molar yield of muconic acid. Finally, we produce materials from three compounds to illustrate the potential for realizing performance-advantaged properties relative to petroleum-derived analogs.

INTRODUCTION

The realization of a vibrant bioeconomy based on conversion of lignocellulose to renewable chemicals and materials will rely on the development of new molecules that exhibit performance-advantaged properties relative to their petroleum-derived counterparts.[1,2] Metabolic pathways across the kingdoms of life have served as a rich source for the engineering of microbial cell factories to produce chemicals across multiple applications, with products derived from central carbon metabolism, isoprenoid, fatty acid, and polyketide synthase pathways among the most thoroughly explored.[1,3,4]

A source of molecular diversity for bioproducts that has been only partially explored to date resides in microbial aromatic catabolism. In nature, some soil microbes funnel aromatic compounds derived from lignin, an abundant aromatic polymer in plants, through diverse "upper pathways" to central aromatic intermediates, including catechol, protocatechuate, and gallate, that subsequently undergo ring-opening.[5] The most thoroughly characterized mechanism of aromatic catabolism employs dioxygenases that utilize oxygen and a metal co-factor to conduct ring-opening via *ortho*- or *meta*-cleavage.[6,7] The ring-opened species

Context & Scale

In the last century, chemicals and materials derived from the byproducts of petroleum production have largely displaced natural products and enabled myriad new applications. Today, fuels, chemicals, and materials derived from plant biomass have the potential to enable innovation and mitigate negative environmental impacts of the petrochemical industry. To achieve this, nature's ability to generate unique molecules with great selectivity could be leveraged to develop new chemicals and materials that would be difficult to access from petroleum and could represent new building blocks for a bio-based materials economy. Here we describe the production of molecules derived from bacterial aromatic catabolic pathways and demonstrate their use in the production of materials with superior properties relative to their petroleum-derived analogs.

are further metabolized through "lower pathways" comprising 4–5 enzymatic steps to generate species that enter central carbon metabolism for energy and growth.[5,6] Figure 1 shows canonical pathways for protocatechuate and catechol catabolism.

Of the intermediates in these pathways (**1**–**16**, See Table S1 for IUPAC names and other identifiers), several have been produced microbially. *cis,cis*-Muconic acid (**16**), the *ortho*-cleavage product of catechol,[8] is a precursor to adipic acid[9] and terephthalic acid[10] and can also be used to produce performance-advantaged materials.[11,12] We and several other groups have demonstrated high titers, rates, and yields of **16** from aromatic compounds in a variety of microbes,[13–18] and seminal work from Draths and Frost demonstrated a route to produce **16** from glucose via the shikimate pathway for aromatic amino acid biosynthesis.[9] While less explored than **16**, 2-pyrone-4,6-dicarboxylic acid (**2**) has been produced from aromatic molecules[19,20] and from glucose using a variation of the Draths and Frost route.[21,22] Bugg and co-workers reported production of two catabolic intermediates from wheat straw that cyclize with ammonia to form dinicotinic acid (**1N**) and isocinchomeronic acid (**10N**),[20] which had been demonstrated previously with 2-hydroxymuconic-semialdehyde (**11**) produced from catechol to form picolinic acid (**11N**).[23] Production of muconolactone (**8**) and β-ketoadipic acid (**9**) from protocatechuate has also been demonstrated.[24] Beyond the compounds produced to date, there are additional molecules between protocatechuate or catechol and central carbon metabolism that exhibit chemical functionality that could enable use as monomers in the development of performance-advantaged chemicals and materials.

Here, we develop strains of the robust aromatic catabolic microbe, *Pseudomonas putida* KT2440, to produce the 15 compounds, beyond **16**, from *ortho*- or *meta*-cleavage of protocatechuate and catechol from model aromatic compounds derivable from lignin. We extend this work by engineering strains to produce **2**, **10N**, **11N**, and **16** from glucose, a readily accessible and commercially established feedstock. We conduct bioreactor cultivations of each strain to baseline product titer, rate, and yield. Bench-scale separations protocols and analytics are developed for each molecule, and three exemplary polymers are produced and characterized from 4-oxalomesaconic acid (enol form) (**3**), **9**, and **10N**. Lastly, techno-economic analysis of **16** is reported to identify key cost drivers toward commercial production of this exemplary product.

RESULTS

Production of the Target Molecules from Aromatic Substrates

Fifteen strains of *P. putida* KT2440 were constructed to contain incomplete pathways for the catabolism of catechol and protocatechuate using genetic deletions and chromosomally integrated gene expression (Figure 1, Table 1, and Tables S2–S5). *P. putida* naturally employs the *ortho*-cleavage pathways for catabolism of protocatechuate and catechol via β-ketoadipate.[5] To accumulate intermediates in this pathway, genes encoding the enzymes that act upon each targeted intermediate (**1**–**9**, Figure 1) were deleted from the *P. putida* genome. Protocatechuate and catechol are metabolized through *meta*-cleavage pathways in other organisms, including *Sphingobium* sp. strain SYK-6 (protocatechuate 4,5 *meta*-cleavage[25]), *Paenibacillus* sp. strain JJ-1b (protocatechuate 2,3 *meta*-cleavage[26]), and *P. putida* mt-2 (catechol *meta*-cleavage[27]). To produce the targeted intermediates in these pathways, the genes encoding the endogenous ring-cleavage dioxygenases that initiate catabolism of protocatechuate (*pcaHG*) and catechol (*catA*/*catA2*) in

[1]National Bioenergy Center, National Renewable Energy Laboratory, Golden, CO 80401, USA

[2]Biosciences Center, National Renewable Energy Laboratory, Golden, CO 80401, USA

[3]Biosciences Division, Oak Ridge National Laboratory, Oak Ridge, TN 37830, USA

[4]Present address: Department of Computer Science, University of Colorado Boulder, Boulder, CO 80309, USA

[5]Present address: Biological Sciences Division, Pacific Northwest National Laboratory, Richland, WA 99354, USA

[6]Present address: GreenLight Biosciences, Inc., Medford, MA 02155, USA

[7]These authors contributed equally

[8]Lead Contact

*Correspondence: gregg.beckham@nrel.gov

https://doi.org/10.1016/j.joule.2019.05.011

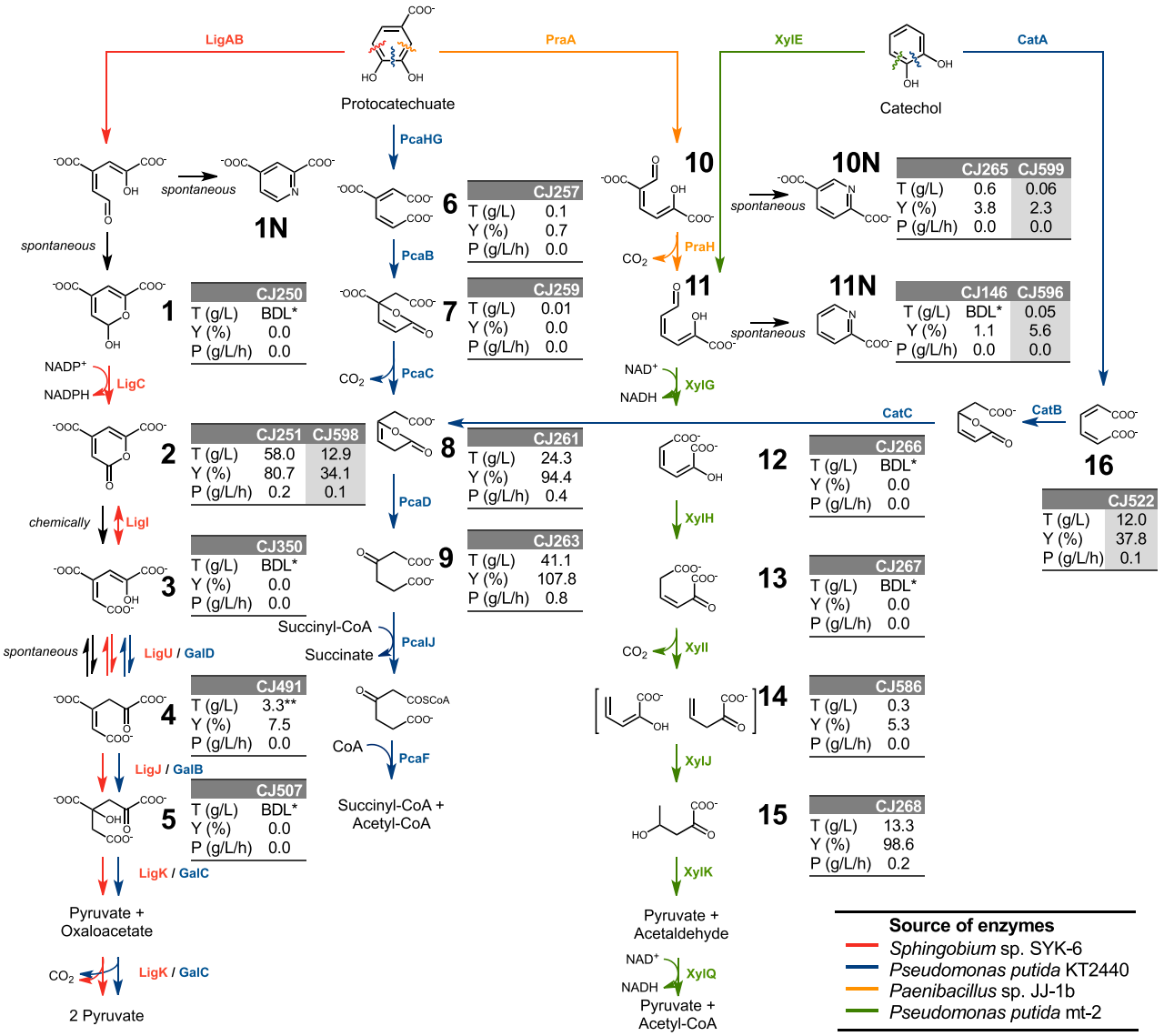

Target molecule identity			
1	4-Carboxy-2-hydroxymuconate-semialdehyde (hemiacetal form)	10	5-Carboxy-2-hydroxymuconate-semialdehyde
1N	Dinicotinic acid	10N	Isocinchomeronic acid
2	2-Pyrone-4,6-dicarboxylic acid	11	2-Hydroxymuconate-semialdehyde
3	4-Oxalomesaconic acid (enol form)	11N	Picolinic acid
4	4-Oxalomesaconic acid (keto form)	12	4-Oxalocrotonic acid (enol form)
5	4-Carboxy-4-hydroxy-2-oxoadipic acid	13	4-Oxalocrotonic acid (keto form)
6	β-Carboxy-*cis*,*cis*-muconic acid	14	2-Hydroxypenta-2,4-dienoic acid / 2-Oxopent-4-enoic acid
7	γ-Carboxymuconolactone	15	4-Hydroxy-2-oxovaleric acid
8	Muconolactone	16	*cis*,*cis*-Muconic acid
9	β-Ketoadipic acid		

Figure 1. Aromatic Catabolic Pathways and the Target Molecules Produced in This Study

The color of the arrows indicates the sources of the enzymes. Adjacent to the targeted compounds, labeled 1–16, are tables with the strain names used for their production and the titers (T), productivities (P), and % yields (mol/mol) (Y) achieved from aromatic compounds (white columns) and glucose (gray columns). The full genotypes of the production strains are included in Table 1. The name for each molecule is also presented at the bottom of the figure. *Indicates that the target compound was below the limit of quantitation but present at detectable levels. **Indicates that CJ491 produced tautomers of 3 and 4.

Table 1. Target Molecules and the Substrates and Strain Genotypes Used for Their Production in This Study

Target	Substrate	Strain	Genotype
1	4-hydroxybenzoate	CJ250	*P. putida* KT2440 Δ*pcaHG*::Ptac:*ligAB*
2	4-hydroxybenzoate	CJ251	*P. putida* KT2440 Δ*pcaHG*::Ptac:*ligABC*
3	4-hydroxybenzoate	CJ350	*P. putida* KT2440 Δ*pcaHG*::Ptac:*ligABCI* Δ*galBCD*
4	4-hydroxybenzoate	CJ507	*P. putida* KT2440 Δ*pcaHG*::Ptac:*ligABCIU* Δ*galBC*::Ptac:*galD*
5	4-hydroxybenzoate	CJ329	*P. putida* KT2440 Δ*pcaHG*::Ptac:*ligABCIUJ* Δ*galC*::Ptac:*galBD*
6	4-hydroxybenzoate	CJ257	*P. putida* KT2440 Δ*pcaBDC*
7	4-hydroxybenzoate	CJ259	*P. putida* KT2440 Δ*pcaDC*
8	4-hydroxybenzoate	CJ261	*P. putida* KT2440 Δ*pcaD*
9	4-hydroxybenzoate	CJ263	*P. putida* KT2440 Δ*pcaIJ*
10/10N	4-hydroxybenzoate	CJ265	*P. putida* KT2440 Δ*pcaHG*::Ptac:*praA*
11/11N	Benzoate	CJ146	*P. putida* KT2440 Δ*catA2* Δ*pcaHG*:: Ptac:*praAH* Δ*catBCA*::Ptac:*xylE*
12	Benzoate	CJ266	*P. putida* KT2440 Δ*catA2* Δ*pcaHG*:: Ptac:*praAH* Δ*catBCA*::Ptac:*xylEG*
13	Benzoate	CJ267	*P. putida* KT2440 Δ*catA2* Δ*pcaHG*:: Ptac:*praAH* Δ*catBCA*::Ptac:*xylEGH*
14	Benzoate	CJ586	*P. putida* KT2440 Δ*catA2* Δ*pcaHG*:: Ptac:*praAH* Δ*catBCA*::Ptac:*xylEGIH*
15	Benzoate	CJ268	*P. putida* KT2440 Δ*catA2* Δ*pcaHG*:: Ptac:*praAH* Δ*catBCA*::Ptac:*xylEGFJIH*
16	Glucose	CJ200	*P. putida* KT2440 Δcat*RBC*::Ptac:*catA* Δ*pcaHG*::Ptac:*aroY*:*ecdB*:*asbF*
16	Glucose	CJ325	*P. putida* KT2440 Δcat*RBC*::Ptac:*catA* Δ*pcaHG*::Ptac:*aroY*:*ecdB*:*asbF* Δ*pykA* Δ*pykF* Δ*ppc*
16	Glucose	CJ385	*P. putida* KT2440 Δcat*RBC*::Ptac:*catA* Δ*pcaHG*::Ptac:*aroY*:*ecdB*:*asbF* Δ*pykA* Δ*pykF* Δ*ppc* Δ*pgi-1* Δ*pgi-2*
16	Glucose	CJ606	*P. putida* KT2440 Δcat*RBC*::Ptac:*catA* Δ*pcaHG*::Ptac:*aroY*:*ecdB*:*asbF* Δ*pykA*::*aroG-D146N*:*aroY*:*ecdB*:*asbF* Δ*pykF* Δ*ppc*
16	Glucose	CJ442	*P. putida* KT2440 Δcat*RBC*::Ptac:*catA* Δ*pcaHG*::Ptac:*aroY*:*ecdB*:*asbF* Δ*pykA*::*aroG-D146N*:*aroY*:*ecdB*:*asbF* Δ*pykF* Δ*ppc* Δ*pgi-1* Δ*pgi-2*
16	Glucose	CJ522	*P. putida* KT2440 Δcat*RBC*::Ptac:*catA* Δ*pcaHG*::Ptac:*aroY*:*ecdB*:*asbF* Δ*pykA*::*aroG-D146N*:*aroY*:*ecdB*:*asbF* Δ*pykF* Δ*ppc* Δ*pgi-1* Δ*pgi-2* Δ*gcd*
2	Glucose	CJ598	*P. putida* KT2440 Δ*pykA*::Ptac:*aroG-D146N*: *asbF* Δ*pykF* Δ*ppc* Δ*pgi-1* Δ*pgi-2* Δ*pcaHG*:: Ptac:*ligABC* Δ*gcd*
10/10N	Glucose	CJ599	*P. putida* KT2440 Δ*pykA*::Ptac:*aroG-D146N*: *asbF* Δ*pykF* Δ*ppc* Δ*pgi-1* Δ*pgi-2* Δ*pcaHG*:: Ptac:*praA* Δ*gcd*
11/11N	Glucose	CJ596	*P. putida* KT2440 Δ*pykA*::Ptac:*aroG-D146N*: *asbF* Δ*pykF* Δ*ppc* Δ*pgi-1* Δ*pgi-2* Δ*pcaHG*:: Ptac:*praAH* Δ*gcd*

P. putida KT2440 were replaced with genes encoding incomplete pathways derived from the species above.[28]

In these strains, a co-substrate such as glucose can be utilized for growth while aromatic substrates are metabolized through pathways that terminate at the desired product. Therefore, shake-flask cultures of these engineered strains were grown on glucose in the presence of 4-hydroxybenzoate or benzoate, which are metabolized via protocatechuate or catechol, respectively, and the supernatants were analyzed by high-performance liquid chromtography (HPLC), positive- and negative-ion electrospray (ESI)-mass spectrometry (MS), tandem mass spectrometry (MS/MS), and nuclear magnetic resonance (NMR) spectroscopy (Figures S1–S8) to determine whether the targets were produced. The targeted molecules were detected in all 15 cases but not quantified due to a lack of commercially available standards for many of the compounds (Table S6). Thus, these molecules were produced in 10-L bioreactors to separate, purify, and use as standards. If the biological production was insufficient, the molecules were synthesized chemically (Schemes S1 and S2). Due to the presence of nitrogen nucleophile in the media, 4-carboxy-2-hydroxymuconate-semialdehyde (hemiacetal form) (**1**), 5-carboxy-2-hydroxymuconate-semialdehyde (**10**), and 2-hydroxymuconate-6-semialdehyde (**11**) spontaneously ring-closed to pyridine molecules **1N**, **10N**, and **11N**[20,29] (Figure 1, Scheme S3), and thus, this form was also analyzed.

For the production of target molecules in bioreactors from aromatic substrates (4-hydroxybenzoate and benzoate), a fed-batch strategy controlled by oxygen saturation was used to add small amounts of aromatic compounds and glucose in each feeding pulse ($\leq$1 mM)[16] to avoid aromatic toxicity and catabolic repression induced by high glucose concentrations.[30] Results were variable among targets (Figures 1 and S9). For instance, **1**, **3**, 4-carboxy-4-hydroxy-2-oxoadipic acid (**5**), 4-oxalocrotonic acid (enol form) (**12**), and 4-oxalocrotonic acid (keto form) (**13**) were not detected in appreciable amounts in the bioreactors. In some of these cases, the substrate and/or metabolic intermediates accumulated (**1**, **12**). In others, the target was not appreciably produced and a major product was not identified, although the substrate was completely utilized (**3**, **5**, **13**). Other molecules were produced at the mg/L scale (β-carboxy-*cis,cis*-muconic acid [**6**], γ-carboxymuconolactone [**7**], **10N**, **11N**, 2-hydroxypenta-2,4-dienoic acid/2-oxopent-4-enoic acid [**14**]). In these cases, the aromatic substrate accumulated during cultivation, even when intermittent feeding containing only glucose was applied to promote substrate utilization. Cultivations to produce 4-oxalo-mesaconic acid (keto form) (**4**) led to the production of high concentrations of a metabolic intermediate, **2** (up to 12 g/L), and tautomers of **3** and **4** (up to 3.3 g/L). Another group of molecules were produced at the g/L scale at yields higher than 80% (mol/mol) (**2**, **8**, **9**, 4-hydroxy-2-oxovaleric acid [**15**]), reaching titers up to 58 g/L (**2**) and productivities of 0.78 g/L/h (**9**). The variability in the performance of these strains likely reflects differences in enzyme kinetics, thermodynamic equilibrium between intermediates, and/or the stability or toxicity of the products or intermediates accumulated.

Production of the Target Molecules from Glucose

Having achieved considerable yields and titers of several targeted compounds from aromatic compounds, we sought to produce a subset of the targeted molecules from glucose, a feedstock that, unlike lignin, is currently available commercially in a form that is bioavailable to the microbe. We recently demonstrated production of **16** from glucose by an engineered *P. putida* strain in which erythrose 4-phosphate (E4P) and phosphoenolpyruvate (PEP) are condensed to form 3-deoxy-D-arabino-

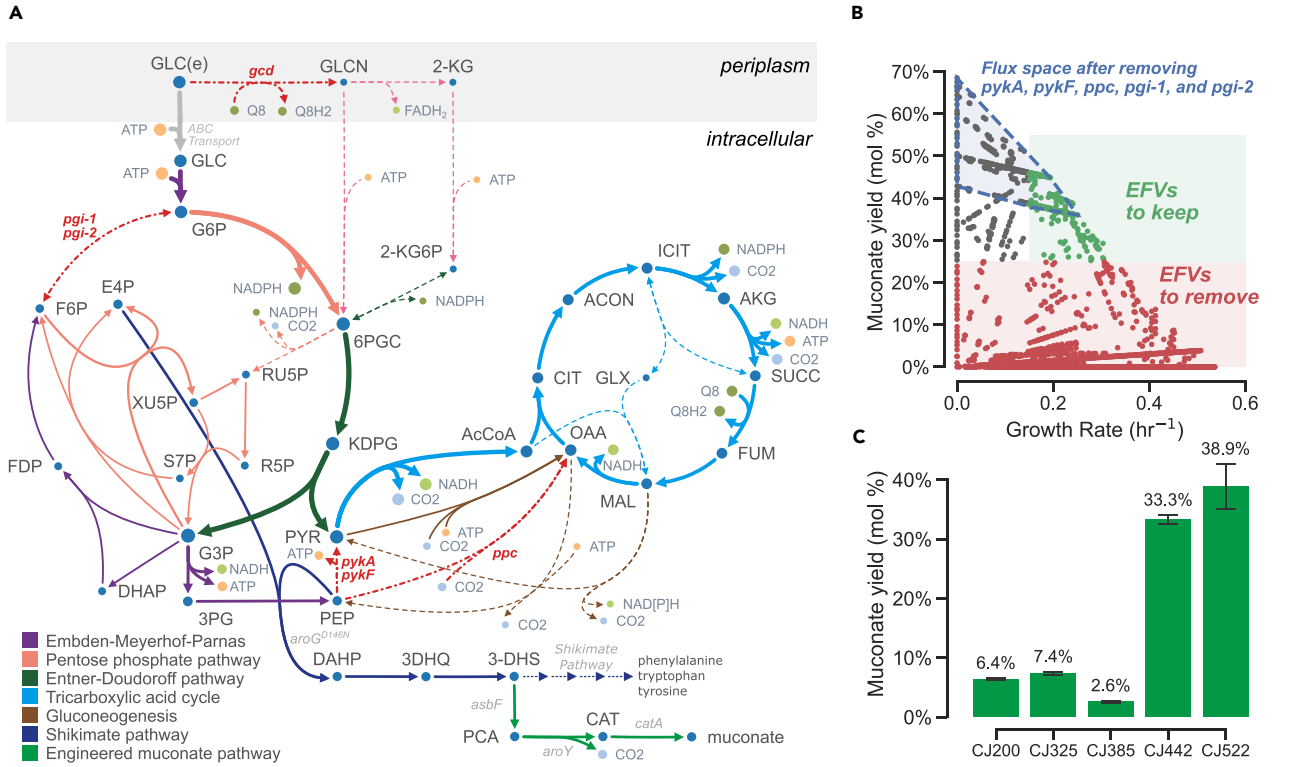

Figure 2. Metabolic Strategy for Production of 16 from Glucose

(A) Metabolic map of *P. putida* KT2440 showing expected fluxes after deletion of *pykA*, *pykF*, *ppc*, *pgi-1*, *pgi-2*, and *gcd*. The model consists of the main pathways for glucose uptake and utilization, including the Embden-Meyerhof-Parnas pathway, the Entner-Doudoroff pathway, the pentose phosphate pathway, the tricarboxylic acid (TCA) cycle, the shikimate pathway, and the **16** production pathway. Dashed lines indicate reactions with no flux. Abbreviations of key metabolites are GLC (glucose), GLCN (gluconate), 2-KG (2-ketogluconate), PYR (pyruvate), PEP (phosphoenolpyruvate), DAHP (3-deoxy-D-arabino-heptulosonate-7-phosphate), 3-DHS (3-dehydroshikimate), PCA (protocatechuate), and CAT (catechol). Full names of all metabolite abbreviations can be found in Table S7. (B) Cut set search strategy. Points represent **16** yield and growth rate from feasible flux solutions. Reaction eliminations were identified that removed all EVFs in red, while keeping at least one mode in green. The flux space after deletion of *pykA*, *pykF*, *ppc*, *pgi-1*, and *pgi-2* is shown in gray, indicating that **16** yield is constrained to be higher than 36% (mol/mol). (C) Yields of **16** (%, mol/mol) from glucose achieved by strains described in this study. Data points represent the average of biological triplicates. Error bars represent the standard deviation of these measurements.

heptulosonate-7-phosphate (DAHP) and enter the shikimate pathway (Figure 2A).[31] Conversion of 3-DHS to **16** is enabled by genome-integrated expression of heterologous genes encoding a 3-dehydroshikimate (3-DHS) dehydratase, AsbF, a protocatechuate decarboxylase, AroY, and EcdB, which synthesizes a prenylated flavin co-factor required by AroY. **16** accumulates in this engineered strain, CJ200, due to deletion of the gene encoding CatB. This strain, however, only achieved a 6.4% ± 0.18% (mol/mol) yield of **16** from glucose (Figures 2C and S11A), far below the theoretical maximum (Supplemental Information Section VIII). Thus, we sought to increase the yield of **16** from glucose by constructing a stoichiometric model of core-carbon metabolism and **16** synthesis in *P. putida* to predict genetic interventions that increase PEP and E4P availability for **16** production while maintaining growth (Data S1). The model was validated by comparing flux predictions to ^{13}C flux measurements for wild-type *P. putida* (Figures S10 and S11 and Table S8).[32] Genetic interventions to increase production of **16** were generated from the model using constrained minimum cut sets (cMCSs)[33] and elementary flux vectors (EFVs).[34] We searched for sets of reaction knockouts that strongly coupled **16** production and biomass synthesis; specifically, high yields (>25% mol/mol) were required for any nonzero flux vector with biomass flux greater than 0.2 (Figure 2B).[35]

The resulting cMCSs consisted of 5 possible knockout sets with 3 reactions each, all of which contained both pyruvate kinase (Pyk) and phosphoenolpyruvate carboxylase (Ppc) (Supplemental Information Section VIII). The *P. putida* genome contains two genes, *pykA* and *pykF*, that encode pyruvate kinases, which convert PEP to pyruvate. Ppc is encoded by a single gene, *ppc*, and allows PEP to enter the TCA cycle via carboxylation to oxaloacetate. Deleting *pykA*, *pykF*, and *ppc* together should block PEP from entering the TCA cycle (Figure 2A). Deletion of these genes from CJ200, generating CJ325, was insufficient to improve **16** yields from glucose in both experimental and modeling results (Figures 2C, S11A, and S11B). Flux balance simulations showed that near-optimal growth rates could be achieved after deletion of *pykA*, *pykF*, and *ppc* by reflux of glyceraldehyde-3-phosphate (G3P) through the EDEMP cycle—a combination of the Entner-Doudoroff (ED) pathway, pentose phosphate (PP) pathway, and gluconeogenicEmbden-Meyerhof-Parnas (EMP) pathway that was recently demonstrated in *P. putida*[32]—to generate pyruvate for entry into the TCA cycle while bypassing PEP. To prevent this, each identified cut set included a third reaction to interrupt the EDEMP pathway. Of the additional targets, elimination of the glucose-6-phosphate isomerases (Pgi) encoded by *pgi-1* and *pgi-2* was selected as the most feasible. Figure 2A shows flux balance predictions for the simultaneous knockout of the genes encoding PykA, PykF, Ppc, Pgi-1, and Pgi-2. These knockouts effectively use the ED pathway to split the incoming carbon into pyruvate, which is metabolized through the TCA cycle, and G3P, which can be used primarily for synthesis of **16**. As indicated by Figure 2B, the selected cut set has a predicted minimum **16** yield of 36.0% (mol/mol) from glucose.

Surprisingly, deletion of *pgi-1*, and *pgi-2* from CJ325, generating CJ385, resulted in a reduction in **16** yield, from 7.4% (mol/mol) to 2.6% (mol/mol) (Figures 2C and S11C). Growth was also diminished (Figure S11C), suggesting that we had successfully interrupted cyclic pyruvate generation via the EDEMP cycle and that carbon was likely available, but carbon flux into the shikimate pathway for **16** production was limited. The shikimate pathway is subject to feedback inhibition by the aromatic amino acids it generates,[36] but feedback-resistant mutants of the DAHP synthase,[37] which catalyzes the irreversible condensation of E4P and PEP, have been used to enhance carbon flux into this pathway.[38,39] We hypothesized that expression of a feedback-resistant DAHP synthase from *E. coli*, AroG^{D146N},[37] and increased expression of the heterologous pathway from 3-DHS to catechol would draw more carbon toward **16** production. Genome integration of an *aroG*^{D146N}*-asbF-aroY-ecdB* gene cassette into CJ385 generated CJ442, which exhibited a 33.3% (mol/mol) yield of **16** from glucose in shake flasks (Figures 2C and S11D).

CJ442 was evaluated in bioreactors in batch and fed-batch modes (Figures 3A, S12A, and S12B) at similar initial glucose concentrations. Yields of **16** reached 30.0% (mol/mol) and 23.0% (mol/mol) in batch and fed-batch mode, respectively (Figures S12A–S12C). In wild-type *P. putida*, approximately 90% of glucose is dehydrogenated to gluconate, of which approximately 10% of that is further converted to 2-ketogluconate (2-KG).[32] These pathways converge at 6-phosphogluconate, which can be further metabolized in the PP or ED pathways (Figure 2A). It was observed that large amounts of 2-KG accumulated when CJ442 was cultivated in a bioreactor (Figure 3A). In batch experiments, 2-KG began to be assimilated following glucose depletion (Figure S12A). In fed-batch mode, where glucose is never depleted, 2-KG accumulated continuously (Figures 3A, S12B, and S12C). Its secretion also results in a reduction in the bioreactor pH that must be neutralized. Thus, we eliminated the conversion of glucose to gluconate and 2-KG by deleting the glucose dehydrogenase gene, *gcd*, from CJ442, generating CJ522. In shake flasks, CJ522 did not accumulate 2-KG and achieved a 38.9%

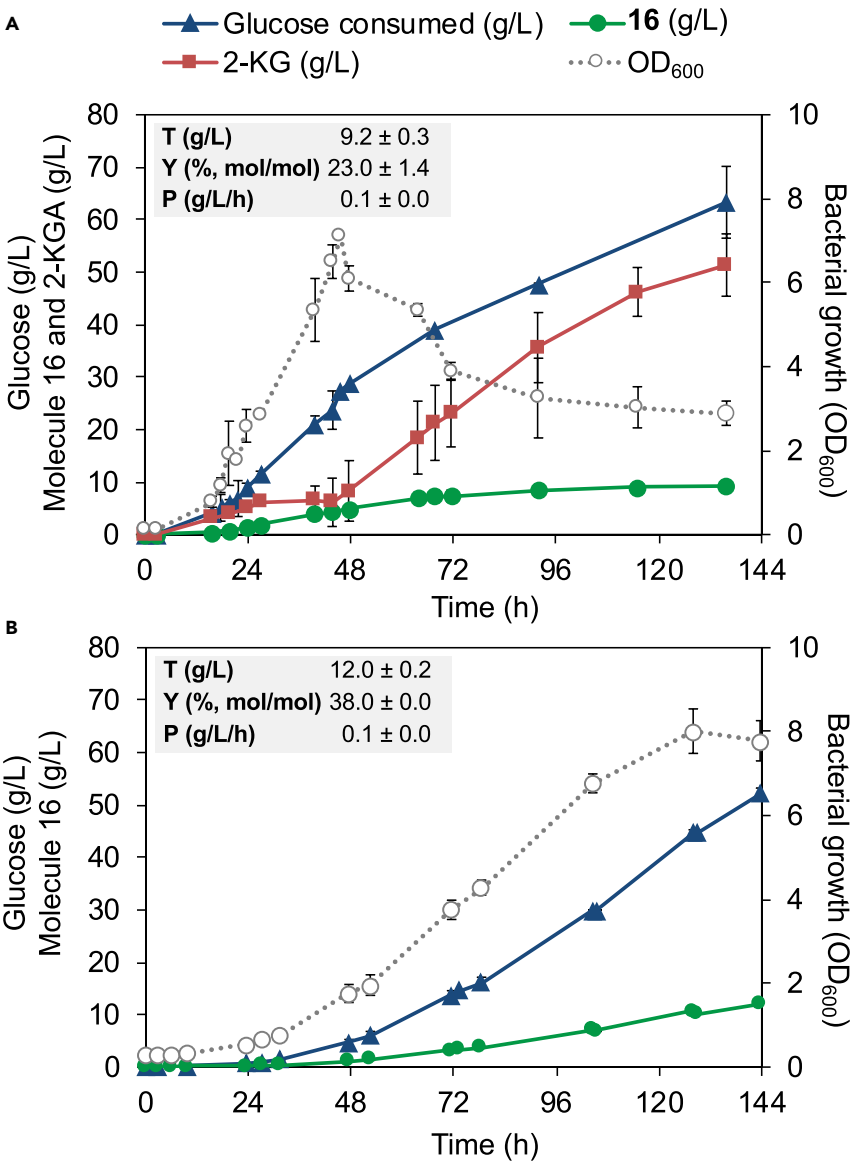

Figure 3. Bioreactor Profiles from Engineered *P. putida* Strains Producing 16 from Glucose in Fed-Batch Mode

(A) Profile from *P. putida* CJ442 cultivations. (B) Profile from *P. putida* CJ522 cultivations. Additional details for these bioreactor experiments are given in Figure S12. Titers (T), yields (Y), and productivity (P) are highlighted for each strain. Titers (g/L) correspond to product concentration at the end of the cultivation time. Yields (%, mol/mol) are calculated as the amount of **16** (in moles) produced (corrected by the dilution factor generated by base and feeding addition) divided by total glucose (in moles) utilized. Productivity (g/L/h) is calculated as product concentration at the last time point divided by the total cultivation time. Data points represent the average of a biological replicate. Error bars represent the absolute difference between the data obtained from the duplicate at each time point. 2-KG, 2-ketogluconate.

(mol/mol) yield (Figures 2C and S11E). When compared in batch (Figure S12D) and fed-batch mode (Figures 3B, S12E, and S12F) bioreactor cultivations, CJ522 achieved **16** yields of 41.3% and 37.8% (mol/mol) from glucose, respectively, 11% and 15% higher than those observed for CJ442. Titers were also slightly higher in CJ522 than CJ442: 12.0 compared to 9.2 g/L.

We then applied the metabolic engineering that enabled **16** production at a high yield from glucose to several other molecules. Specifically, we deleted *pykA*, *pykF*, *ppc*, *pgi-1*, *pgi-2*, and *gcd* and integrated genes encoding AsbF and AroG^{D146N} into strains engineered to produce **2**, **10N**, and **11N**, generating strains CJ598, CJ599, and CJ596, respectively. These strains were evaluated in fed-batch bioreactor cultivations (Figure S13). CJ598 produced 12.9 g/L of **2** at a yield of 34%, and a productivity of 0.09 g/L/h, similar to the titer, yield, and productivity achieved for **16** by CJ522 in fed-batch mode. CJ596 produced a mixture of **10N** and **11N** at low titers (<0.1 g/L). CJ599, which was engineered to produce **10N**, instead produced 0.7 g/L of **11N** at a yield of 35.3%. It has been suggested that **10** may undergo spontaneous abiotic decarboxylation to **11**.[40]

Polymerization of Select Target Molecules Generates Performance-Advantaged Materials

Subsequently, we developed separation methods from the bioreactor broths (Table S9 and Scheme S4) and explored the potential of a subset of the targeted compounds as polymer precursors. To access a tricarboxylic acid at appreciable quantities, **2** was chemically converted to **3** via facile reflux in water (Scheme S1). **3** was reacted with 1,8-diaminooctane at a 3× molar excess to generate microspheres with a diameter between 0.1 μm and 100 μm. After separation by dialysis, the spheres were uniform in size, exhibiting an average diameter of 0.2 μm (Figure 4A), a suitable size for use in agricultural extended release applications,[41] theranostics in biomedical applications,[42] and as a modifier and filler in polymer composites.[43]

While biological production of **1N** and **10N** presented challenges, these aromatic dicarboxylic acids represent potential alternatives to terephthalic acid. Polyethylene terephthalate (PET) analogs were generated using **1N** or **10N** by converting these compounds to their acyl chloride monomers and to the bis(2-hydroxyethyl) (BHE) analogs. The BHE analogs of these monomers were transesterified to produce high-molecular-weight polymers. The PET-analog made using **10N** was compared to PET because of the crystalline nature and structural similarity between the two polymers. Due to their structural similarity, this analog and PET possess very similar thermal properties and permeabilities (Figure 4B), but the analog possesses a heteroatom that can enable further modification and applications beyond those of PET, such as conducting polymers for fuel cells. The **1N** PET analog resembles amorphous PET (Table S10).

β-ketoadipic acid, **9**, is a diacid that can be reacted with hexamethyl diamine (HMDA) to produce a polyamide analogous to nylon 6,6 (Figure 4C and Scheme S6). Due to its β-ketone functionality, however, **9** can spontaneously decarboxylate during polymerization (Scheme S5). To avoid this, **9** was converted to an acyl chloride. The polyamide synthesized from **9** exhibits a higher molecular weight, glass transition temperature, and melting temperature than nylon 6,6 synthesized from adipic acid under the same conditions. These increases in melting point and crystallinity lead to a reduction in water uptake in the **9**-derived nylon, a key limitation in the incumbent, nylon 6,6 (Table S11).

Techno-Economic Analysis of 16 and Adipic Acid Production from Glucose and Lignin

For less-explored biosynthetic pathways, techno-economic analysis (TEA) can be a useful tool to identify key cost drivers at an early stage to inform further research. Thus, TEA was conducted to estimate the minimum selling price (MSP) from glucose and lignin of two exemplary products from this study, namely **16**, or adipic acid generated by catalytic hydrogenation of **16**. Adipic acid was selected to illustrate

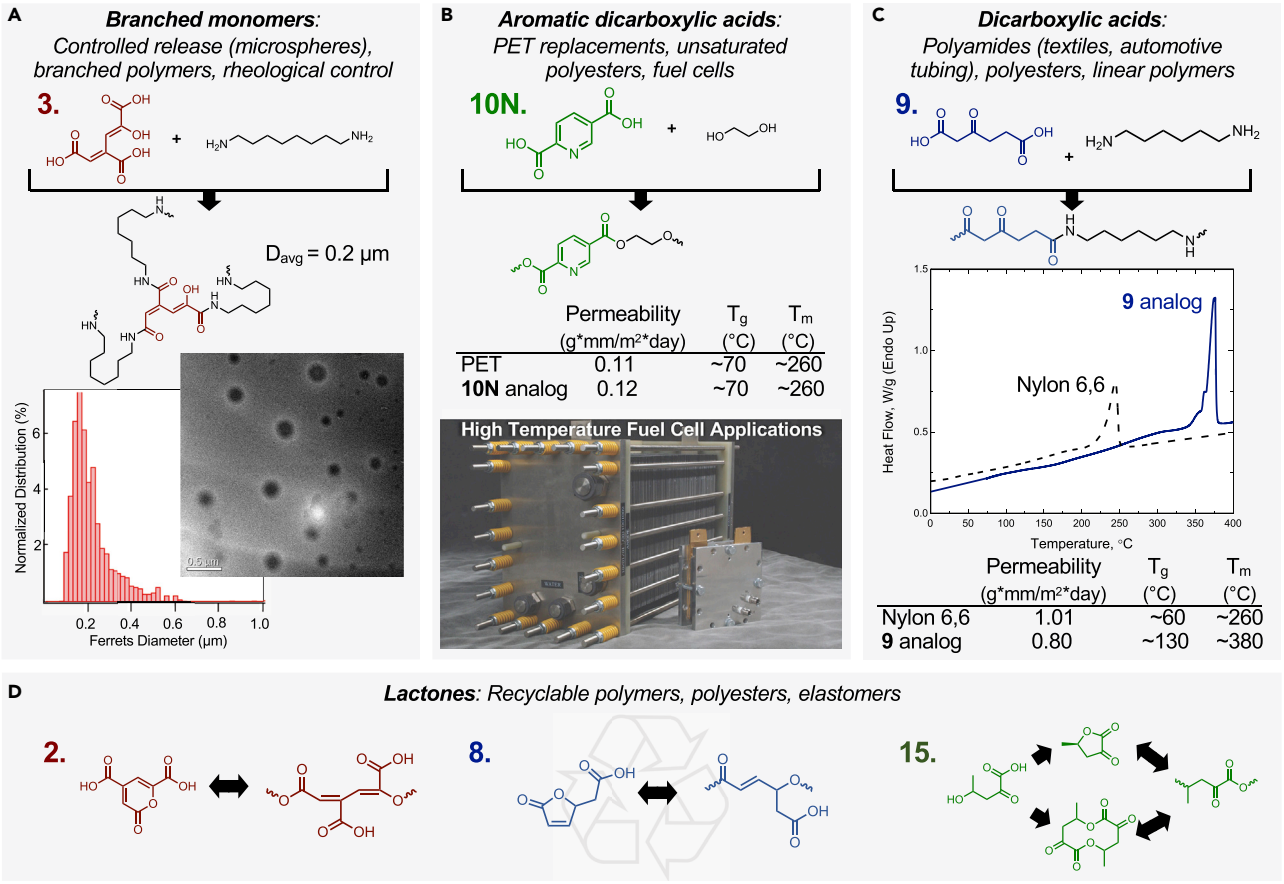

Figure 4. Potential Polymer Platforms in which Target Molecules Can Be Employed as Either Functional Replacements or Performance-Advantaged Materials

(A) The reaction of a tricarboxylic acid **3** with diamines to form microspheres. (B) Condensation of **10** with ethylene glycol to synthesize a functional PET analog, and fuel cell visualization. (C) Reaction of **9** with hexamethyl diamine to form a nylon with performance-differentiated properties (solid blue line and text) from nylon 6,6 (dotted black line and text), namely a higher T_g, T_m, and lower permeability. (D) The three lactones, **2**, **8**, and **15**, in this pathway that can undergo ring-opening polymerization. Lactones are inherently recyclable and thus provide performance-advantaged behavior. Thermal measurements have an associated error of ±3°C.

a pathway to a drop-in replacement and enable direct comparison with a fossil-derived chemical product that has an existing market. Using first-generation sugars at a price of $0.27/kg and 40% MA yield, we assessed a facility slated to produce 100.8 MM kg/year of **16** or 102.5 MM kg/year of adipic acid. For adipic acid, this production capacity would account for ~3.7% of the annual market of 3 million tons.[44,45] The operating conditions are provided in Tables S12–S14 and Figure S14, with the economic inputs detailed in Tables S15–S18. The process flow diagram is shown in Figure S15. From first-generation sugars, the model predicts an MSP of $1.95/kg for MA and $2.13/kg for adipic acid (Table S19). For comparison, the average market price of adipic acid in 2017 was $1.80/kg.[46] Capital costs are dominated by the aerobic bioreactors, and operating costs by the feedstock requirements (Table S20 and Figures S16 and S17).

Sensitivity analyses were also conducted to evaluate the effects of rate, yield, and feedstock type. These results demonstrated that productivity must be increased to 0.5 g/L/h, above which gains in MSP diminish, and yield, as expected for a bioprocess, is a major cost driver (Figure S18). Transitioning to second-generation

lignocellulosic sugars with an assumed price of $0.40/kg increases the predicted MSP for adipic acid by $0.48/kg (Figure S19). Transitioning to lignin monomers, with an assumed price of $0.04/kg based on the energy value, decreases the **16** and adipic acid MSPs to $0.86/kg and $1.05/kg, respectively. Overall, the TEA highlights that **16** productivity from sugars must be improved and that lignin as a feedstock could enable a dramatic reduction in product MSP, given the substantially higher theoretical atom efficiency relative to production of **16** from glucose.

DISCUSSION

Concerns over global climate change have catalyzed growing demand for sustainable, biologically derived replacements for chemicals and materials traditionally produced from petroleum. Synthetic biology approaches have the potential to source direct replacements for petrochemical-derived monomers used in incumbent materials such as nylon 6,6 and PET, which can be derived from **16**. In addition, increasing attention has been placed on "bioprivileged" molecules, such as **16**, that also possess useful functionalities that could enable their use in the production of materials with novel or performance-advantaged properties and that are more readily accessible from bio-based feedstocks than petrochemicals.[2,11,12] Such molecules are of interest for their potential to enable development of new materials and applications that provide sustainable solutions to address the demand and performance requirements of existing and new markets, innovation that has stalled as the petrochemical industry has matured.

We posit that, in addition to **16**, the 15 other intermediates in aromatic catabolism examined here also have potential as bioprivileged molecules in applications including homopolymers, copolymers, composites,[11] and fuel cell membranes.[47] In particular, the proposed platform has the potential to generate polymer precursors with oxygenated functionality, such as ketones and lactones, that cannot be easily accessed via petrochemical routes. Ketones can lend advantaged properties by inducing crystallinity,[48] while lactones can be used to introduce control of polymer architecture (e.g., block copolymers) and recyclability[49] (Figure 4D). The carboxylic acids in these compounds can be catalytically converted to esters, alcohols, acrylates, or nitriles.[50] Nitrogen can also be introduced via ammonia-induced ring-closure (**1N**, **10N**, **11N**). Further control is afforded by either branched monomers—which can be produced at high titers via **3** and that enable rheological control when incorporated into backbones[51]—and olefinic-containing monomers (most notably **16**) that can undergo radical or ionic polymerization in a polymer backbone to produce crosslinked materials. Overall, this unique functionality can enable thermoplastics and thermosets with controllable properties to be synthesized from biomass.

Relative to other biological-derived targets such as alcohols, fatty-acids, polyketides, and terpenoids, aromatic catabolic intermediates exhibit several advantages. In particular, these molecules are derived from catabolic pathways, which are intrinsically less regulated and biologically expensive than the biosynthetic pathways required to generate fatty acids, polyketides, and terpenoids—products the cell tends to produce as needed. Because these catabolic pathways are situated above central carbon metabolism, they are subject to less CO_2 loss and, thus, are more atom efficient relative to many bio-derived targets. Finally, these molecules are derived from linear pathways, making engineering strains for their production relatively simple compared to targets that also serve as precursors for other essential components of the cell, that are intermediates in bifurcated pathways, or that

require the condensation of two or more intermediates that would, ideally, be generated in exact stoichiometries.

Some of the advantages discussed above apply to these compounds only when they are produced from lignin-derived aromatics. Progress has been made toward the production of **16** from lignin,[13,15,16,18] and research in this area continues. Ultimately, commercially relevant production of these targets from real lignin will require development of technologies and infrastructure that do not exist at industrial scale today.[52] In the near term, the aromatic catabolic intermediates could be viable targets for production from first-generation sugars. Using model-driven strain engineering, a feedback insensitive DAHP synthase,[37] and a previously described artificial pathway linking the shikimate pathway to the aromatic catabolic pathways,[9] we achieved production of molecule **16** with a 41.3% yield (mol/mol) from glucose. This represents a substantial improvement from 30%, the highest yield reported previously, to our knowledge, for any biological system.[8] Importantly, this has been achieved without the use of plasmid-based gene expression or auxotrophic mutations that require the supplementation of antibiotics and/or other nutrients that would be inconsistent with industrial-scale production of a commodity chemical.

Additional engineering or evolution of the strains described here could improve production by removing bottlenecks to increase conversion rates or increasing the tolerance to toxic products. Additional bioprocess development could also be applied to increase the titers, yields, and productivities of strains evaluated here. Adjustments to the feeding strategy (e.g., glucose/aromatic compound ratio, duration, or mode) and/or bioreactor setup (e.g., high-cell density or *in situ* product recovery, etc.) can lead to important process improvements. Increasing titers would also alleviate some of the difficulties associated with separations, but further separations development is needed for the molecules examined here. For example, **9** in the free acid form rapidly decarboxylates to levulinic acid. **1N**, **10N**, and **11N** are difficult to separate as the nitrogen protonates before the carboxylic acid when acidified to form the free acid. All molecules in the present work, but specifically **9**, **1N**, **10N**, and **11N**, are ideal targets for ionic resin-based separations. Overall, TEA can be utilized to co-design bioprocesses and downstream processing to reduce the MSP, and directions for further improvements are presented here.

In summary, this work demonstrates production of intermediates of bacterial aromatic catabolic pathways and their potential as building blocks for performance-advantaged materials. We developed strains derived from *P. putida* KT2440 to produce these molecules from lignin-derived aromatic molecules and from glucose, in some cases at high yields and titers. Methods to quantify and separate these molecules were also developed and demonstrated. We illustrated the potential utility of these chemically diverse molecules as building blocks for new materials by polymerizing several of them to generate materials with unique, and in some cases superior, properties relative to their incumbent analogs, work that could be extended to myriad applications and markets.

EXPERIMENTAL PROCEDURES

All materials and methods are provided in the Supplemental Information.

SUPPLEMENTAL INFORMATION

Supplemental Information can be found online at https://doi.org/10.1016/j.joule.2019.05.011.

ACKNOWLEDGMENTS

This work was partially authored by Alliance for Sustainable Energy, LLC, the manager and operator of the National Renewable Energy Laboratory for the U.S. Department of Energy under Contract No. DE-AC36-08GO28308. Oak Ridge National Laboratory is managed by UT-Battelle, LLC, for the U.S. DOE under contract DE-AC05-00OR22725. We acknowledge funding from NREL Laboratory Directed Research and Development (LDRD) program. Support is also acknowledged from the U.S. Department of Energy, Office of Energy Efficiency and Renewable Energy, Bioenergy Technologies Office via the Agile BioFoundry project for the development of strains CJ442 and CJ522 and techno-economic analysis. G.T.B. acknowledges partial support from the Center for Bioenergy Innovation, a U.S. Department of Energy Research Center supported by the Office of Biological and Environmental Research in the DOE Office of Science. Support for N.A.R. was partially provided by the U.S. Department of Energy, Office of Science, Office of Workforce Development for Teachers and Scientists, Office of Science Graduate Student Research (SCGSR) program. The SCGSR program is administered by the Oak Ridge Institute for Science and Education for the DOE under contract number DE-AC05-06OR23100. Funding for C.R.M. was provided by the Colorado College Riley Scholar-in-Residence program for research support. We thank Sandra Notonier for use of her plasmid, pSN2, in strain construction and Eric Karp for helpful discussions on separations.

AUTHOR CONTRIBUTIONS

C.W.J., D.R.V., and G.T.B. conceived of the project. C.W.J., G.D., J.R.E., P.K., and A.M.G. conducted the metabolic engineering. D.S., P.S., T.A.V., and X.Y. conducted the bioreactor cultivations. N.A.R. and C.R.M. conducted the separations. N.A.R., C.R.M., and A.N.W. performed the polymer synthesis. B.A.B., N.S.C., W.E.M., D.J.P., and K.J.R. conducted the analytics. D.R.V., N.G., and M.J.B. conducted the techno-economic analysis. P.C.S.J. and Y.J.B. performed the metabolic modeling. C.W.J., D.S., N.A.R., B.A.B., D.R.V., P.C.S.J., and G.T.B. wrote the manuscript with critical input from all authors.

DECLARATION OF INTERESTS

C.W.J., D.S., P.C.S.J., D.R.V., J.R.E., A.M.G., and G.T.B. hold patents and have submitted patent applications on engineered strains related to this work. N.A.R., D.R.V., and G.T.B. have submitted patent applications on the production of polymers from these molecules.

Received: March 20, 2019
Revised: April 27, 2019
Accepted: May 13, 2019
Published: May 20, 2019

REFERENCES

1. Zhu, Y., Romain, C., and Williams, C.K. (2016). Sustainable polymers from renewable resources. Nature *540*, 354–362.

2. Shanks, B.H., and Keeling, P.L. (2017). Bioprivileged molecules: creating value from biomass. Green Chem. *19*, 3177–3185.

3. Jang, Y.-S., Kim, B., Shin, J.H., Choi, Y.J., Choi, S., Song, C.W., Lee, J., Park, H.G., and Lee, S.Y. (2012). Bio-based production of C2-C6 platform chemicals. Biotechnol. Bioeng. *109*, 2437–2459.

4. Peralta-Yahya, P.P., Zhang, F., del Cardayre, S.B., and Keasling, J.D. (2012). Microbial engineering for the production of advanced biofuels. Nature *488*, 320–328.

5. Harwood, C.S., and Parales, R.E. (1996). The beta-ketoadipate pathway and the biology of self-identity. Annu. Rev. Microbiol. *50*, 553–590.

6. Fuchs, G., Boll, M., and Heider, J. (2011). Microbial degradation of aromatic compounds - from one strategy to four. Nat. Rev. Microbiol. *9*, 803–816.

7. Vaillancourt, F.H., Bolin, J.T., and Eltis, L.D. (2006). The ins and outs of ring-cleaving dioxygenases. Crit. Rev. Biochem. Mol. Biol. *41*, 241–267.

8. Xie, N.-Z., Liang, H., Huang, R.-B., and Xu, P. (2014). Biotechnological production of muconic acid: current status and future prospects. Biotechnol. Adv. *32*, 615–622.

9. Draths, K.M., and Frost, J.W. (1994). Environmentally compatible synthesis of adipic acid from D-glucose. J. Am. Chem. Soc. *116*, 399–400.

10. Lu, R., Lu, F., Chen, J., Yu, W., Huang, Q., Zhang, J., and Xu, J. (2016). Production of diethyl terephthalate from biomass-derived muconic acid. Angew. Chem. Int. Ed. Engl. *55*, 249–253.

11. Rorrer, N.A., Vardon, D.R., Dorgan, J.R., Gjersing, E.J., and Beckham, G.T. (2017). Biomass-derived monomers for performance-differentiated fiber reinforced polymer composites. Green Chem. *19*, 2812–2825.

12. Suastegui, M., Matthiesen, J.E., Carraher, J.M., Hernandez, N., Rodriguez Quiroz, N., Okerlund, A., Cochran, E.W., Shao, Z., and Tessonnier, J.-P. (2016). Combining metabolic engineering and electrocatalysis: application to the production of polyamides from sugar. Angew. Chem. Int. Ed. Engl. *55*, 2368–2373.

13. Becker, J., Kuhl, M., Kohlstedt, M., Starck, S., and Wittmann, C. (2018). Metabolic engineering of *Corynebacterium glutamicum* for the production of *cis, cis*-muconic acid from lignin. Microb. Cell Fact. *17*, 115.

14. van Duuren, J.B.J.H., Wijte, D., Leprince, A., Karge, B., Puchałka, J., Wery, J., Dos Santos, V.A., Eggink, G., and Mars, A.E. (2011). Generation of a *catR* deficient mutant of *P. putida* KT2440 that produces *cis, cis*-muconate from benzoate at high rate and yield. J. Biotechnol. *156*, 163–172.

15. Kohlstedt, M., Starck, S., Barton, N., Stolzenberger, J., Selzer, M., Mehlmann, K., Schneider, R., Pleissner, D., Rinkel, J., Dickschat, J.S., et al. (2018). From lignin to nylon: Cascaded chemical and biochemical conversion using metabolically engineered *Pseudomonas putida*. Metab. Eng. *47*, 279–293.

16. Salvachúa, D., Johnson, C.W., Singer, C.A., Rohrer, H., Peterson, D.J., Black, B.A., Knapp, A., and Beckham, G.T. (2018). Bioprocess development for muconic acid production from aromatic compounds and lignin. Green Chem. *20*, 5007–5019.

17. Sonoki, T., Takahashi, K., Sugita, H., Hatamura, M., Azuma, Y., Sato, T., Suzuki, S., Kamimura, N., and Masai, E. (2017). Glucose-free *cis,cis*-muconic acid production via new metabolic designs corresponding to the heterogeneity of lignin. ACS Sustainable Chem. Eng. *6*, 1256–1264.

18. Vardon, D.R., Franden, M.A., Johnson, C.W., Karp, E.M., Guarnieri, M.T., Linger, J.G., Salm, M.J., Strathmann, T.J., and Beckham, G.T. (2015). Adipic acid production from lignin. Energy Environ. Sci. *8*, 617–628.

19. Otsuka, Y., Nakamura, M., Shigehara, K., Sugimura, K., Masai, E., Ohara, S., and Katayama, Y. (2006). Efficient production of 2-pyrone 4,6-dicarboxylic acid as a novel polymer-based material from protocatechuate by microbial function. Appl. Microbiol. Biotechnol. *71*, 608–614.

20. Mycroft, Z., Gomis, M., Mines, P., Law, P., and Bugg, T.D.H. (2015). Biocatalytic conversion of lignin to aromatic dicarboxylic acids in *Rhodococcus jostii* RHA1 by re-routing aromatic degradation pathways. Green Chem. *17*, 4974–4979.

21. Luo, Z.W., Kim, W.J., and Lee, S.Y. (2018). Metabolic engineering of escherichia coli for efficient production of 2-pyrone-4,6-dicarboxylic acid from glucose. ACS Synth. Biol. *7*, 2296–2307.

22. Michinobu, T., Hishida, M., Sato, M., Katayama, Y., Masai, E., Nakamura, M., Otsuka, Y., Ohara, S., and Shigehara, K. (2007). Polyesters of 2-pyrone-4,6-dicarboxylic acid (PDC) obtained from a metabolic intermediate of lignin. Polym. J. *40*, 68–75.

23. Asano, T., Ukita, Y., Matsui, K., Takeo, M., Negoro, S., and Utsumi, Y. (2006). Fabrication of a micro reactor for vertical unit operation using multifunctional fluid filter and its application to biochemical reaction. Microsyst. Technol. *13*, 441–446.

24. Okamura-Abe, Y., Abe, T., Nishimura, K., Kawata, Y., Sato-Izawa, K., Otsuka, Y., Nakamura, M., Kajita, S., Masai, E., Sonoki, T., and Katayama, Y. (2016). Beta-ketoadipic acid and muconolactone production from a lignin-related aromatic compound through the protocatechuate 3,4-metabolic pathway. J. Biosci. Bioeng. *121*, 652–658.

25. Kamimura, N., Takahashi, K., Mori, K., Araki, T., Fujita, M., Higuchi, Y., and Masai, E. (2017). Bacterial catabolism of lignin-derived aromatics: New findings in a recent decade: Update on bacterial lignin catabolism. Environ. Microbiol. Rep. *9*, 679–705.

26. Kasai, D., Fujinami, T., Abe, T., Mase, K., Katayama, Y., Fukuda, M., and Masai, E. (2009). Uncovering the protocatechuate 2,3-cleavage pathway genes. J. Bacteriol. *191*, 6758–6768.

27. Franklin, F.C., Bagdasarian, M., Bagdasarian, M.M., and Timmis, K.N. (1981). Molecular and functional analysis of the TOL plasmid pWWO from *Pseudomonas putida* and cloning of genes for the entire regulated aromatic ring meta cleavage pathway. Proc. Natl. Acad. Sci. USA *78*, 7458–7462.

28. Johnson, C.W., and Beckham, G.T. (2015). Aromatic catabolic pathway selection for optimal production of pyruvate and lactate from lignin. Metab. Eng. *28*, 240–247.

29. Shindo, K., Osawa, A., Nakamura, R., Kagiyama, Y., Sakuda, S., Shizuri, Y., Furukawa, K., and Misawa, N. (2004). Conversion from arenes having a benzene ring to those having a picolinic acid by simple growing cell reactions using *Escherichia coli* that expressed the six bacterial genes involved in biphenyl catabolism. J. Am. Chem. Soc. *126*, 15042–15043.

30. Johnson, C.W., Abraham, P.E., Linger, J.G., Khanna, P., Hettich, R.L., and Beckham, G.T. (2017). Eliminating a global regulator of carbon catabolite repression enhances the conversion of aromatic lignin monomers to muconate in *Pseudomonas putida* KT2440. Metab. Eng. Commun. *5*, 19–25.

31. Johnson, C.W., Salvachúa, D., Khanna, P., Smith, H., Peterson, D.J., and Beckham, G.T. (2016). Enhancing muconic acid production from glucose and lignin-derived aromatic compounds via increased protocatechuate decarboxylase activity. Metab. Eng. Commun. *3*, 111–119.

32. Nikel, P.I., Chavarría, M., Fuhrer, T., Sauer, U., and de Lorenzo, V. (2015). *Pseudomonas putida* KT2440 strain metabolizes glucose through a cycle formed by enzymes of the Entner-Doudoroff, Embden-Meyerhof-Parnas, and pentose phosphate pathways. J. Biol. Chem. *290*, 25920–25932.

33. Jungreuthmayer, C., Nair, G., Klamt, S., and Zanghellini, J. (2013). Comparison and improvement of algorithms for computing minimal cut sets. BMC Bioinformatics *14*, 318.

34. Klamt, S., Regensburger, G., Gerstl, M.P., Jungreuthmayer, C., Schuster, S., Mahadevan, R., Zanghellini, J., and Müller, S. (2017). From elementary flux modes to elementary flux vectors: Metabolic pathway analysis with arbitrary linear flux constraints. PLoS Comput. Biol. *13*, e1005409–e1005422.

35. Klamt, S., and Mahadevan, R. (2015). On the feasibility of growth-coupled product synthesis in microbial strains. Metab. Eng. *30*, 166–178.

36. Herrmann, K.M., and Weaver, L.M. (1999). The shikimate pathway. Annu. Rev. Plant Physiol. Plant Mol. Biol. *50*, 473–503.

37. Kikuchi, Y., Tsujimoto, K., and Kurahashi, O. (1997). Mutational analysis of the feedback sites of phenylalanine-sensitive 3-deoxy-D-arabino-heptulosonate-7-phosphate synthase of *Escherichia coli*. Appl. Environ. Microbiol. *63*, 761–762.

38. Draths, K.M., Pompliano, D.L., Conley, D.L., Frost, J.W., Berry, A., Disbrow, G.L., Staversky, R.J., and Lievense, J.C. (1992). Biocatalytic synthesis of aromatics from D-glucose: the role of transketolase. J. Am. Chem. Soc. *114*, 3956–3962.

39. Lütke-Eversloh, T., and Stephanopoulos, G. (2007). L-tyrosine production by deregulated strains of *Escherichia coli*. Appl. Microbiol. Biotechnol. *75*, 103–110.

40. Crawford, R.L., Bromley, J.W., and Perkins-Olson, P.E. (1979). Catabolism of protocatechuate by *Bacillus macerans*. Appl. Environ. Microbiol. *37*, 614–618.

41. Li, Y., Zhou, M., Pang, Y., and Qiu, X. (2017). Lignin-based microsphere: preparation and performance on encapsulating the pesticide avermectin. ACS Sustainable Chem. Eng. *5*, 3321–3328.

42. Wang, Y., Shim, M.S., Levinson, N.S., Sung, H.-W., and Xia, Y. (2014). Stimuli-responsive materials for controlled release of theranostic agents. Adv. Funct. Mater. *24*, 4206–4220.

43. Friedrich, K., Zhang, Z., and Schlarb, A.K. (2005). Effects of various fillers on the sliding wear of polymer composites. Compos. Sci. Technol. *65*, 2329–2343.

44. Biddy, M.J., Scarlata, C., and Kinchin, C. (2016). Chemicals from biomass: a market assessment of bioproducts with near-term potential (National Renewable Energy Laboratory). https://www.nrel.gov/docs/fy16osti/65509.pdf.

45. Davis, R., Grundl, N., Tao, L., Biddy, M.J., Tan, E.C.D., Beckham, G.T., Humbird, D., Thompson, D.N., and Roni, M.S. (2018). Process Design and Economics for the Conversion of Lignocellulosic Biomass to Hydrocarbon Fuels and Coproducts: 2018 Biochemical Design Case Update: Biochemical Deconstruction and Conversion of Biomass to Fuels and Products via Integrated Biorefinery Pathways (National Renewable Energy Laboratory). https://www.nrel.gov/docs/fy19osti/71949.pdf.

46. Gunukula, S., Runge, T., and Anex, R. (2017). Assessment of biocatalytic production parameters to determine economic and environmental viability. ACS Sustainable Chem. Eng. *5*, 8119–8126.

47. Xiao, L., Zhang, H., Jana, T., Scanlon, E., Chen, R., Choe, E.W., Ramanathan, L.S., Yu, S., and Benicewicz, B.C. (2005). Synthesis and characterization of pyridine-based polybenzimidazoles for high temperature polymer electrolyte membrane fuel cell applications. Fuel Cells *5*, 287–295.

48. Holt, G.A., and Spruiell, J.E. (2002). Melting and crystallization behavior of aliphatic polyketones. J. Appl. Polym. Sci. *83*, 2124–2142.

49. Schneiderman, D.K., and Hillmyer, M.A. (2017). 50th anniversary perspective: There is a great future in sustainable polymers. Macromolecules *50*, 3733–3749.

50. Karp, E.M., Eaton, T.R., Sànchez I Nogué, V., Vorotnikov, V., Biddy, M.J., Tan, E.C.D., Brandner, D.G., Cywar, R.M., Liu, R., Manker, L.P., et al. (2017). Renewable acrylonitrile production. Science *358*, 1307–1310.

51. Wang, L., Jing, X., Cheng, H., Hu, X., Yang, L., and Huang, Y. (2012). Rheology and crystallization of long-chain branched poly(L-lactide)s with controlled branch length. Ind. Eng. Chem. Res. *51*, 10731–10741.

52. Beckham, G.T., Johnson, C.W., Karp, E.M., Salvachúa, D., and Vardon, D.R. (2016). Opportunities and challenges in biological lignin valorization. Curr. Opin. Biotechnol. *42*, 40–53.